ACS Catalysis

Letter

pubs.acs.org/acscatalysis

Bulk Hydrodesulfurization Catalyst Obtained by $Mo(CO)_6$ Grafting on the Metal−Organic Framework Ni_2(2,5-dihydroxoterephthalate)

Cherif Larabi,[†] Pia Kjær Nielsen,[‡,§] Stig Helveg,[‡] Chloé Thieuleux,[†] Frank B. Johansson,*[,‡] Michael Brorson,*[,‡] and Elsje Alessandra Quadrelli*[,†]

[†]Université de Lyon, ICL, UMR 5265 (CNRS−CPE Lyon−Université Lyon 1), Bât 308F, 43 Boulevard du 11 Novembre 1918, 69616 Villeurbanne, France

[‡]Haldor Topsøe A/S, Nymøllevej 55, DK-2800 Kgs, Lyngby, Denmark

[§]Department of Physics and Chemistry, University of Southern Denmark, Campusvej 55, DK-5230 Odense M, Denmark

Supporting Information

ABSTRACT: The Metal−Organic Framework, $[Ni_2(dhtp)]$ (H_4dhtp = 2,5-dihydroxyterephthalic acid) was modified by gas-phase grafting of $Mo(CO)_6$ at the gram-scale via a post-synthesis modification approach. A highly dispersed well-defined bimetallic material containing the $[Ni_2(dhtp)Mo(CO)_3]$ fragment either in the staggered or in the eclipsed conformation was obtained, with a maximum coverage of 50%$_{mol}$, as shown by multitechnique characterization: IR (diagnostic ν(CO) = 1996, 1972, 1926, 1885, and 1797 cm^{-1}), N_2 adsorption (Brunauer−Emmett−Teller (BET) surface area = 172 m^2 g^{-1}, pore volume 0.1 cm^3/g), elemental analyses (Ni = 21.6%$_{wt}$, Mo = 9.6%$_{wt}$), mass balanced analyses of evolved gases (3.0 ± 0.2 mols of CO evolved/mol of grafted $Mo(CO)_6$ high-resolution transmission electron microscopy (HRTEM). The staggered conformer is stabilized by an intermolecular Ni···(OC)Mo interaction with the framework open Ni(II) site, which causes the markedly blue-shifted stretching band observed at ν(CO) = 1797 cm^{-1}. Upon decomposition in dihydrogen−hydrogen sulfide at 350 °C (p_{H2} = 50 bar), the resulting bulk material is a heterogeneous catalyst for hydrodesulfurization (HDS). The HDS activity of the catalyst was based on the average measured conversion of dibenzothiophene to biphenyl (BP) or cyclohexylbenzene (CHB) by online calibrated GC-MS analyses under steady state conditions and converted to the corresponding relative pseudo first-order rate constants [k(HDS) = k(BP) + k(CHB)]. The activity of the MOF-generated material is markedly superior to the reference bulk unsupported HDS catalysts $NiMoO_4$ (pseudo first-order rate k(HDS) = 30 vs 14 h^{-1}) while containing 4 time less molybdenum (wt % = 10 vs 44). Activities on hydrodenitrogenation (HDN) and hydrogenation (HYD) are also reported. Analysis by HRTEM and X-ray diffraction (XRD) of the spent catalyst and comparison with model systems revealed well-formed MoS_2 nanoparticles (average sheet thickness 25 Å, corresponding to about 4 stacked layers of MoS_2 sheets, the MoS_2 (011) interlayer distance being 6.15 Å). The presence of Ni in the MoS_2 particles was inferred by the lack of HDS activity of the nickel-free material obtained from analogous chemisorption of $Mo(CO)_6$ in isostructural Zn analogue followed by the same in situ sulfidation procedure.

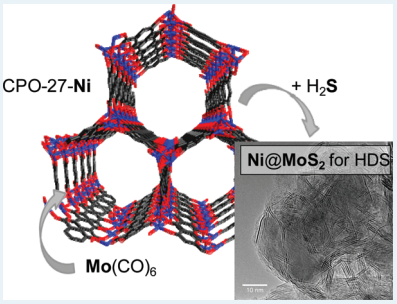

KEYWORDS: *HDS, heterogeneous catalysts, MOF, CPO-27-Ni, Ni-MOF-74, molybdenum, nickel*

Hydrodesulfurization (HDS) is the oil refinery process for removal of sulfur from sulfur-containing organics present in crude oil fractions. The process typically relies on alumina-supported heterogeneous catalysts (>100,000 ton/y) with molybdenum−cobalt or molybdenum−nickel sulfides together constituting the active component.[1] The catalytically active Co−Mo−S or Ni−Mo−S nanoparticles are obtained by in situ sulfidation of the transition metal oxide precursor material present on the alumina surface.[2−4] Alumina provides mechanical robustness to the catalyst particles and secures a high dispersion of the active phase. For example, unsupported Ni−Mo-S prepared from bulk $NiMoO_4$ displays only 10−20% HDS activity of the alumina-supported catalysts; such drop in activity is mainly associated with the low dispersion of the final Ni−Mo−S nanoparticles achieved from sulfidation of the bulk oxide precursor in the absence of support. At the same time, Al_2O_3 ends up constituting 70−80 wt % of the alumina-supported catalyst weight without playing a catalytic role per se. Since the use of unsupported HDS catalysts would circumvent this issue, novel ways to achieve good dispersion of the active Ni−Mo−S phase using a bulk NiMo precursor while avoiding use of a support such as alumina are sought. In this quest for bulk HDS catalyst, we turned to metal−organic frameworks (MOFs),[5−9] which have sparked, among other applications, considerable interest as novel catalytic materials.[9−17]

We report herein the application of the well-defined MOF $[Ni_2(dhtp)]$[18] (H_4dhtp = 2,5-dihydroxyterephthalic acid), a member of the isostructural CPO-27-M[19] and M-MOF-74[20]

Received: October 13, 2011
Revised: March 14, 2012
Published: March 15, 2012

series, as precursor to catalytically active, bimetallic nickel-containing molybdenum sulfide nanoparticles. The second metal, molybdenum, is introduced in the MOF pore structure by post-synthetic modification (PSM)[21,22] via $Mo(CO)_6$ sublimation into the pores and chemical grafting by surface organometallic chemistry.[23] The final sulfidation of all transition metals present in the MOF is achieved by high-temperature treatment with H_2S/H_2 and leads to a break down of the MOF crystal structure; the MOF may thus be considered as a sacrificial part in the synthesis of the final bimetallic NiMo particles, as previously shown only for monometallic Pt nanoparticles obtained from MOF-5 impregnated with Pt salts.[24] We will also report the catalytic performances of such bimetallic sulfided nanoparticles in HDS. MOFs and functionalized MOFs have already been used in the context of HDS, either as precursors for sorbent materials of organo-sulfur compounds[25−28] or as HDS catalyst per se.[29,30] In these latter reports specifically mentioning HDS,[29,30] as well as in other catalytic applications of MOFs,[9−14] the functionalized MOFs are assumed to maintain their hybrid organic−inorganic structures during the catalytic process, while the here reported use of MOF as a templating medium to fully inorganic catalysts has little if any precedent.

RESULTS SECTION

The active material was prepared by subliming $Mo(CO)_6$ on activated $[Ni_2(dhtp)]$,[18] which is characterized, inter alia, by a large Ni content (24 wt %), high surface area (Langmuir surface area of 1083 $m^2\ g^{-1}$ and a pore volume of 0.41 $cm^3\ g^{-1}$), permanent porosity upon desolvation,[31] open Ni(II) sites upon activation,[31−34] and capacity of grafting metal carbonyls such as $Cr(CO)_6$ on the dihydroxoterephthalate linker to yield $[(dhtp)Cr(CO)_3]$ species.[35] The typical synthesis consisted in four sublimation cycles of $Mo(CO)_6$ on activated porous $[Ni_2(dhtp)]$, obtained by prior treatment of the MOF at 120 °C under vacuum (10^{-5} Torr) overnight. Each cycle was followed by gentle thermal treatment (1 h, 120 °C) in a two-vessel self-contained reactor, and a final dynamic vacuum desorption step.

To establish the maximum coverage for well-defined grafting, samples **1**−**5** were prepared by exposing $[Ni_2(dhtp)]$ to increasing $Mo(CO)_6$ quantities; initial $Mo(CO)_6$: $[Ni_2(dhtp)]$ ratio = 0.2, 0.4, 0.6, 0.8, and 1.0 for samples **1**−**5**, respectively. Inductively coupled plasma atomic emission spectrometry (ICP AES) analysis of the final molybdenum and nickel contents in the five samples showed that the Mo uptake by $[Ni_2(dhtp)]$ is quantitative up to a maximum Mo/dhtp molar ratio of 0.5 in the post-synthesis modified material (i.e., Mo_{MAX} = 9.6 wt %, see Figure 1). This is approximately reached at the composition of sample **3**. For materials **1**−**3**, in situ IR measurement of the CO released during the grafting procedure established the evolution of 3.0 ± 0.2 mols of CO/mol of grafted $Mo(CO)_6$ (Supporting Information, Table S1), confirming that the expected grafting stoichiometry (eq 1) is occurring on the quasi totality of the functionalized sites, unlike the previously observed formation of subcarbonyls obtained when a different grafting route is followed:[35]

$$[Ni_2(dhtp)] + Mo(CO)_6 \rightarrow [Ni_2(dhtp)Mo(CO)_3] + 3CO \quad (1)$$

The IR spectra of materials **1**−**5** (Figure 1) show the ν(CO) stretching bands of the surface chemisorbed species $[(dhtp)Mo(CO)_3]$, both in eclipsed conformation (major conformation) with a triplet at 1996, 1885, and 1797 cm^{-1} (assigned in

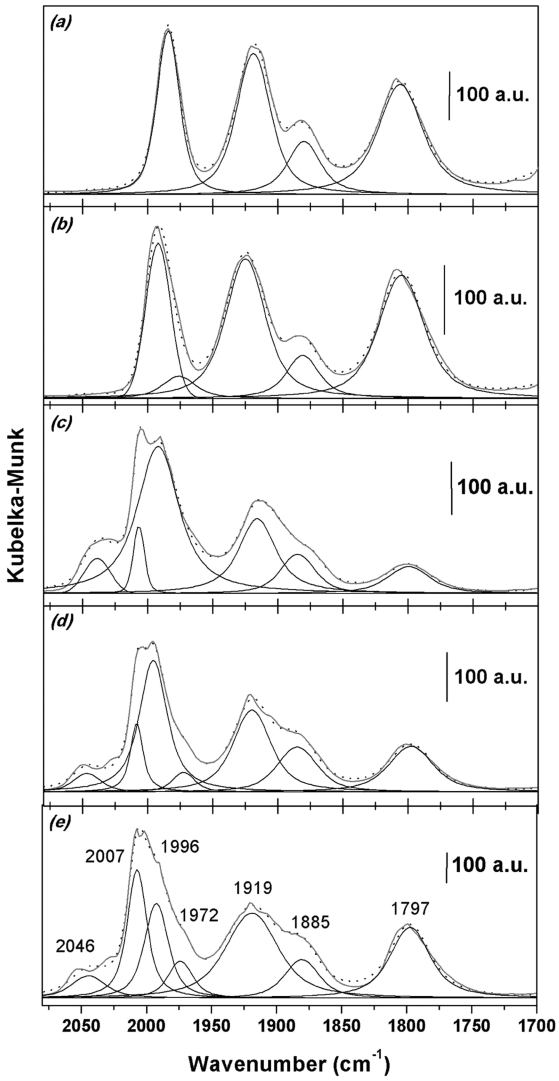

Figure 1. Top: FT-IR of ν(CO) region of the materials **1**−**5** obtained by subliming $Mo(CO)_6$ on $[Ni_2(dhtp)]$ with starting Mo:dhtp molar ratio of (a) 20%, (b) 40%, (c) 60%, (d) 80%, and (e) 100%. The solid line is the experimental spectrum and the dashed line is the composed one from the deconvolution using 7 Gaussian functions fixed at 2046, 2007, 1996, 1972, 1919, 1885, and 1797 on the cm^{-1} scale. **Bottom**: Experimental molybdenum content determined by the ICP AES in samples **1**−**5** vs the theoretical maximum molybdenum content assuming full grafting of the $Mo(CO)_6$ introduced into the sublimation reactor.

dx.doi.org/10.1021/cs200530e | ACS Catal. 2012, 2, 695−700

analogy with the triplet calculated[36] and observed[35] for the chromium analogue [(dhtp)Cr(CO)$_3$] in CPO-27-Ni/Ni-MOF-74) and in the staggered conformation (minor conformation) with a doublet at 1972 and 1926 cm^{-1}, based on the assignment reported by Kaye and Long[37] for the same molecular fragment [(arene)Mo(CO)$_3$] in the MOF-5 framework. The absence of the 1972 cm^{-1} component in the deconvolution spectra of samples **1** and **3** is explained by the fact that in the experimental spectra the low intensity 1972 cm^{-1} absorption amounts to a shoulder of the main peak at 1996 cm^{-1} (Figures 1a and 1c) and hence vanishes in the deconvolution treatment. The observed blue-shifted triplet observed for the eclipsed conformer has been theoretically explained[36] in terms of the close interaction of carbonyl ligands with Ni Lewis sites, an interaction that is exclusive to the eclipsed conformer in the Ni-MOF framework (Scheme 1), and

Scheme 1. Staggered (Left) and Eclipsed (Right) Conformers of [Ni$_2$(dhtp)Mo(CO)$_3$] Surface Fragment Identified by IR Spectroscopy in Samples 1−5

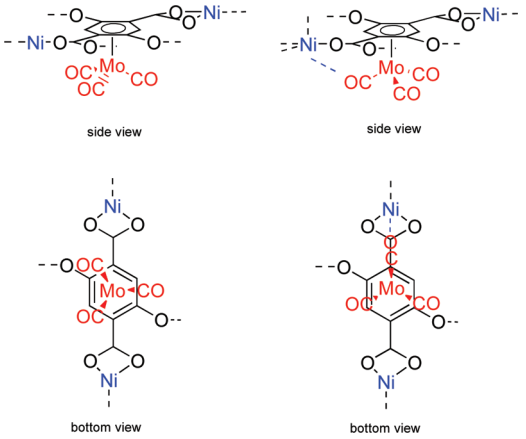

which is expected to stabilize the grafted Mo(CO)$_3$ fragment inside the MOF.[36] The IR spectra of high-loading samples **3**−**5** (≈10 wt % Mo) show weak T_{1u} and E_g vibrational modes of Mo(CO)$_6$ at 2007 and 2046 cm^{-1}, indicating that traces of physisorbed molybdenum hexacarbonyl species have remained in samples prepared from an excess amount of Mo(CO)$_6$. The material is stable under vacuum: no molybdenum loss other than physisorbed Mo(CO)$_6$ is observed when longer desorption steps are performed. Subcarbonyl species observed when employing other post-synthesis modification routes for depositing Mo(CO)$_6$ on [Ni$_2$(dhtp)][35] are not detected for the present large-scale four-cycle grafting protocol. In summary, the combined microanalysis-IR spectroscopy study indicates that close-vessel chemical vapor deposition of Mo(CO)$_6$ on [Ni$_2$(dhtp)] leads to the strongly bonded well-defined surface organometallic species [(dhtp)Mo(CO)$_3$], present in two conformers (eclipsed and staggered), and whose total content is maximized on material **3**, where half of the phenyl rings of the starting MOF are functionalized, corresponding to the stoichiometry [Ni$_2$(dhtp)Mo$_{0.5}$(CO)$_{1.5}$].

N$_2$ adsorption and X-ray diffraction (XRD) analyses of **3** show that material remains porous (Brunauer−Emmett−Teller (BET) area = 172 m^2 g^{-1}, pore volume = 0.1 cm^3/g) and crystalline after grafting post-synthesis modification of [Ni$_2$(dhtp)]. The drop in pore volume (0.1 vs 0.41 cm^3/g in the starting [Ni$_2$(dhtp)] material) and the similar drop in surface area clearly confirm that a substantial amount of the pore space is occupied by the grafted Mo(CO)$_3$ fragments. The material stability during thermal treatment under vacuum is novel with respect to previous reports,[35] and is expected to favor the Mo−Ni codispersion during the in situ activation described hereafter.

The porous, highly dispersed, bimetallic Ni−Mo material **3** was used as precursor to a HDS catalyst. HDS catalysts operate industrially at hydrogen pressures between 30 and 120 bar and temperatures in the range 250−400 °C, precise conditions depending on the nature of the oil feed and the required product specifications. A realistic test of new materials must therefore be conducted at these pressures and temperatures. In the laboratory, conditions similar to those employed at oil-refineries can be realized by means of either a fixed bed reactor where the oil feed and hydrogen flows through a heated bed of the solid catalyst particles or in a slurry-bed reactor where the catalyst particles are continuously stirred in oil and in the presence of hydrogen. We have chosen to employ a fixed-bed setup for the study of MOF materials since this allows simpler online analysis of the product stream by means of gas chromatography. Also, since the MOFs are intended only as precursors to the active HDS catalyst, the fixed-bed reactor allows a convenient in situ transformation into the active phase before the actual catalytic test is conducted; the precursor can be exposed to a stream of sulfiding feed, and any decomposition products formed during activation of the catalysts are removed from the catalyst bed by the flow. In a typical catalytic test, after having loaded the pelletized and granulated material **3** in the high-pressure fixed-bed reactor, the material was sulfided for 4 h at 350 °C by reaction with H_2S in the presence of 42 atm H_2. Then, the activity of the now activated catalyst material was measured at 350 °C in the presence of 38 atm H_2. Because of the complexity of mineral oil in terms of hydrocarbon matrix and the various sulfur compounds present, real oil was not used in these screening experiments. Instead, oil was modeled (as before[38,39]) by an *n*-heptane solution containing dibenzothiophene (3 wt %) as a representative sulfur compound, indole (0.5 wt %), and naphthalene (1 wt %), as representatives, respectively, for the many nitrogen and aromatic compounds that are co-converted with sulfur compounds in the industrial process. To keep the catalyst in a fully sulfided state during the activity measurements, dimethyldisulfide (2.5 wt %) was also present in the model feed as a convenient source of H_2S by thermal decomposition. At reaction conditions all feed and product components are in the gaseous state. The activities of the catalyst for the HDS, hydrodenitrogenation (HDN), and hydrogenation (HYD) reactions of Scheme 2 were measured after reaching the steady state and repeated 8 times. The given activities are based on the average measured conversion by online calibrated GC-MS analyses and converted to the corresponding relative pseudo first-order rate constants, k(HDS) = k(BP) + k(CHB), k(HDN), and k(HYD) (Table 1). A supported reference NiMo/Al$_2$O$_3$ catalyst and bulk NiMoO$_4$ were measured in the same way for comparison.

The MOF-derived sulfided material (**3-H$_2$S**) resulted to be an active bulk HDS catalyst, stable over several cycles (see Experimental Methods part). As reported in Table 1, its activity was almost twice the HDS activity of the reference unsupported bulk material NiMoO$_4$ [k(HDS) = 30 vs 14], while containing four times less molybdenum by weight [wt %(Mo) = 10 vs 44], yielding almost an order of magnitude improvement in the

dx.doi.org/10.1021/cs200530e | ACS Catal. 2012, 2, 695−700

Scheme 2. Model Oil Catalytic Hydrotreating Reactions Taking Place at 350°C and $p(H_2)$ = 38 atm over the Sulfided Catalyst Samples[a]

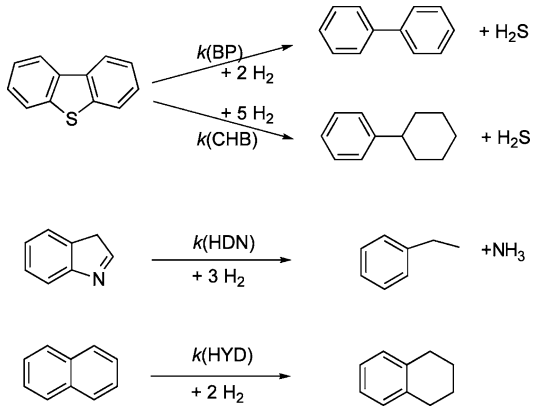

[a]There are two pathways for HDS of dibenzothiophene, and the overall rate constant for HDS, k(HDS), is the sum of k(BP) and k(CHB).

Table 1. Pseudo First-Order Rate Constants for HDS, HDN, and HYD Reactions[a] Determined for Bulk $NiMoO_4$, for the MOF-Derived Material 3 and for a Supported $NiMo/Al_2O_3$ Reference Catalyst Prepared as Industrial Catalysts[b]

materials	wt % Mo	k(HDS) h^{-1}	k(HDN) h^{-1}	k(HYD) h^{-1}
$NiMoO_4$ (bulk)	44	14	20	9
3, $[Ni_2(dhtp)Mo_{0.5}(CO)_{1.5}]$	10	30	31	16
$NiMo/Al_2O_3$ (reference)	17	108	69	59

[a]cf. Scheme 2. [b]All materials were sulfided in situ in the high-pressure reactor before measurement of the catalytic activity (see text).

catalytic activity per molybdenum center [k(HDS): wt %(Mo) = 3.0 vs 0.31]. The HDN and HYD activities are also relatively large for **3-H_2S**. In comparison with the alumina-supported reference catalyst, the activity of the MOF-derived catalyst **3-H_2S** still leaves something to be desired [k(HDS): wt %(Mo) = 3 vs 8], but can be considered promising, since the MOF based system is not yet optimized. Furthermore, the activity is very good for HDN in particular even with respect to the alumina-supported catalyst $NiMo/Al_2O_3$, considering the low metal content of **3** [k(HDN): wt %(Mo) = 3.1 vs 5].

After the activity measurements, **3-H_2S** was retrieved from the reactor and characterized. Powder XRD shows microcrystallites (>0.1 μm) of Ni_2S_3 and nanocrystallites of MoS_2 (average sheet thickness 25 Å), possibly in the presence of amorphous carbon that could be formed during the thermal treatment of the MOF precursor **3**.[40] The thickness of the MoS_2 crystallites suggests an average of about 4 stacked layers of MoS_2 sheets per crystallite in reasonable agreement with Figure 2 (see below). While the Ni_2S_3 phase is catalytically irrelevant and a common byproduct of sulfidation steps in HDS technology,[1] the observed MoS_2-phase constitutes the HDS active Ni−Mo−S phase[1] (whose Ni atoms are not detectable by XRD, but are inferred by the very low activity of the material derived from $Mo(CO)_6$@Zn-MOF, vide infra). High-resolution transmission electron microscopy (HRTEM) micrographs show a characteristic line structure with an interspacing of 0.615 nm, which is attributed to layered (Ni-)Mo−S sheets oriented with their (001) basal plane along the electron beam direction (Figure 2).

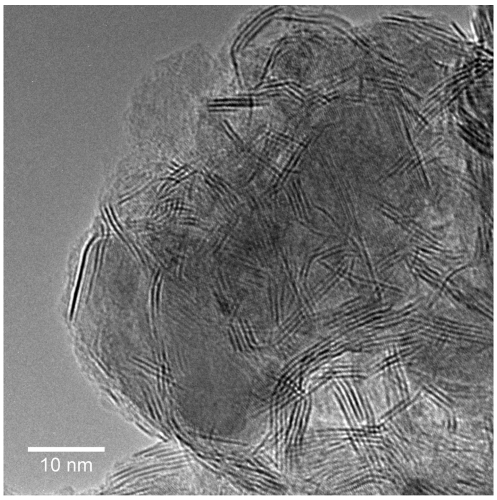

Figure 2. High-resolution TEM image of MOF-derived catalyst **3-H_2S** after activity test. The MOF framework is completely decomposed and the line structure with an interspacing of 0.615 nm is attributed to MoS_2 structures (composed of S−Mo−S layers), imaged "edge-on" with varying stacking heights.

For comparison, the alumina-supported reference catalyst is characterized by extremely dispersed, and thus highly active, 1 or 2 layer-high MoS_2 nanocrystallites,[1] while the $NiMoO_4$-derived catalyst is characterized by more than 8 layer-high MoS_2 stacks (XRD estimated thickness 51 Å, see Supporting Information, Figure S3), in line with the lower activity observed for $NiMoO_4$.

The catalytically essential edge-decoration of MoS_2 nanocrystallites by Ni atoms is not observable in the present images. For high catalytic activity the combination of both Ni promoter and the MoS_2 phase is important.[1] This was confirmed by measurement of the catalytic activities of MOF-derived catalysts obtained by either grafting $Cr(CO)_6$ on Ni_2(dhtp) or by grafting $Mo(CO)_6$ on Zn_2(dhtp).[19] Neither of these materials would be expected[1] to have any substantial activities after sulfidation and indeed all pseudo rate constants were found to be <1 h^{-1}, that is, 0 within the estimated accuracy of the measurement, therefore indirectly confirming the nickel presence in the MoS_2 crystallites obtained from **3**.

In conclusion, we have shown that a porous MOF may serve as a vehicle in obtaining very dispersed, catalytically active metal-containing nanoparticles. In particular, we have here reported how the high degree of nickel atom dispersion in [Ni_2(dhtp)] and the similarly high degree of molybdenum atom dispersion in the post-synthesis modified MOF containing grafted molybdenum carbonyl appear to be a very attractive starting point for forming HDS catalytically active bimetallic (Ni)Mo−S nanoparticles. It will be insightful to explore how the size and shape of the initial MOF crystallites determine the size and activity of final catalytically active material. Such contribution would help establish the structure activity correlation between the sacrificial MOF templating material and the final inorganic catalytically active phase. Work is ongoing aiming at increasing the molybdenum coverage in the MOF to further improve the catalytic activity of the final catalyst.

dx.doi.org/10.1021/cs200530e | ACS Catal. 2012, 2, 695−700

EXPERIMENTAL METHODS

Large Scale Procedure for Grafting of $Mo(CO)_6$ on Ni_2(dhtp) and IR Characterization. Prior to reaction with the metal hexacarbonyls, loose ochre powder of CPO-27-Ni, $[Ni_2(dhtp)]$,[18] was activated under vacuum (10^{-5} Torr) at 393 K overnight and loaded under argon atmosphere in a glass reactor containing a stirring magnet. $Mo(CO)_6$ was loaded in another glass reactor (see Supporting Information, Table S1 for quantities). The two reactors were connected, and the argon was evacuated, after cooling the molybdenum-containing reactor in liquid nitrogen bath. By removal of the liquid nitrogen, the hexacarbonyl was allowed to diffuse into the other reactor. The MOF powder, now under hexacarbonyl atmosphere, was stirred and heated at 120 °C for 3 h. After cooling back at room temperature, the volatiles were condensed back in the molybdenum containing reactor with a liquid nitrogen bath. The sublimation/reaction/desorption cycle was repeated 4 times, each time the quantity of desorbed white crystallites, attributed to unreacted $Mo(CO)_6$ diminished. By the end of the cycles, excess white crystallites, if any, were removed at 120 °C under dynamic vacuum.The samples **1**−**5** were recovered as ochre powder and analyzed by DRIFT (see Figure 1).

Precatalyst Conditioning and Sulfidation. After pelletization (1.5 ton/cm^2) and insertion of the materials in the fixed bed reactor (600−800 μm sieve fraction, see Supporting Information for more details), the sulfidation was carried out in the presence of pressurized hydrogen (total pressure 50 bar) by a feed flow containing dimethyldisulfide, Me_2S_2, dissolved in *n*-heptane contacted with the catalyst precursor for 4 h at 350 °C, where Me_2S_2 decomposition in the presence of H_2 creates the necessary partial pressure of H_2S.

Catalytic Tests. The model oil used is composed of 3% dibenzothiophene (DBT), 0.5% indole, 1% naphtalene, 2.5% dimethyldisulfide (DMDS), 0.5% *n*-nonane (used as internal standard for the gas chromatographic analysis), the rest being *n*-heptane solvent. The catalytic tests were carried out using a fixed-bed reactor operated at feed flow 0.3 mL/min, H_2 flow 250 N mL/min, pressure 50 bar, temp. 350 °C. A test performed on a precatalyst prepared with simple impregnation of $Mo(CO)_6$ on $[Ni_2(dhtp)]$ showed very little Mo incorporation and almost no catalytic activity. Likewise, a sample prepared by exposure of an activated $[Ni_2(dhtp)]$ to vapor pressure of $Mo(CO)_6$ followed by vacuum treatment[35] failed to produce an active catalyst.

Determination of Activity. Upon exit from the reactor, the gaseous product is injected into a GC that records a chromatogram. This chromatogram contains signals for both unconverted reactants and for the products formed, previously assigned by GC-MS. Since both reactants and products are being measured, the method comprises a test of mass balance for every reactant/product pair. Mass balances have been found to be very good. For each of the 3 reactants (A) a pseudo first-order rate constant is calculated based on the measured conversion (0% < conv. < 100%):

$$\ln\left(\frac{[A]}{[A]_0}\right) = -kt$$

$$\Leftrightarrow \ln\left(\frac{[A]_0 - \mathrm{conv}[A]_0}{[A]_0}\right) = -kt$$

$$\Leftrightarrow \ln(1 - \mathrm{conv}) = -kt$$

At steady state conditions the catalyst produces a product stream of steady composition. The time t parameter in the first-order kinetic equation is therefore the residence time of the feed in the reactor. This residence time is equal to the reciprocal Weight Hourly Space Velocity (WHSV) defined as:

$$\mathrm{WHSV} = \frac{\mathrm{Flow} \times \mathrm{feed\ density}}{\mathrm{catalyst\ mass}}$$

We thus get:

$$k = -\mathrm{WHSV} \times \ln(1 - \mathrm{conv})$$

Variation of Catalyst Activity over Time. Each catalyst test involves first an activation/sulfidation step in which the catalyst is exposed to a feed containing only DMDS in *n*-heptane for 4 h. Then a shift to the actual feed takes place, and after a 4 h stabilization period, a total of 8 GC analyses of the product stream are made every 60 min. For each point in time the catalytic activity is calculated. Since our catalysts do not deactivate (e.g., by sintering of catalytically active structures or deposition of carbonaceous material on top of active structure), the activity is constant in time, and the pseudo first-order rate constant can be reported as an average of the 8 measurements.

Characterization of Materials. The electron microscopy measurements were carried out on a Titan microscope operated at 300 kV in microprobe mode, see Supporting Information for more details.

ASSOCIATED CONTENT

Supporting Information

Apparatus, chemical analysis, grafting protocol, CO release quantification, FT-IR spectra, textural characterization, precatalyst sulfidation, activity measurements in high-pressure reactor, and powder XRD diagrams. This material is available free of charge via the Internet at http://pubs.acs.org.

AUTHOR INFORMATION

Corresponding Author

*Fax: +45 4527 2999 (M.B.), (F.B.J.), +33472431795 (E.A.Q.). Phone: +45 4527 2000 (M.B.), (F.B.J.), +33426237159 (E.A.Q.). E-mail: frbj@topsoe.dk (F.B.J.), mib@topsoe.dk (M.B.), quadrelli@cpe.fr (E.A.Q.).

Funding

This work was carried out with funding from EU under the NMP programme (Contract No NMP4-CT-2006-033335, MOFCAT project).

Notes

The authors declare no competing financial interest.

ACKNOWLEDGMENTS

Jean-Marie Basset and Tarun Maishal are gratefully acknowledged for preliminary data and useful discussion on large-scale $Cr(CO)_6$ grafting on $[Ni_2(dhtp)]$.

REFERENCES

(1) *Hydrotreating Catalysis, Science and Technology*; Topsøe, H., Clausen, B. S., Massoth, F. E., Eds.; Springer-Verlag: Berlin, Germany, 1996.

(2) Helveg, S.; Lauritsen, J. V.; Laegsgaard, E.; Stensgaard, I.; Norskov, J. K.; Clausen, B. S.; Topsøe, H.; Besenbacher, F. *Phys. Rev. Lett.* **2000**, *84*, 951−954.

(3) Hinnemann, B.; Moses, P. G.; Noerskov, J. K. *J. Phys.: Condens. Matter* **2008**, *20*, 064236/1−064236/8.

(4) Topsøe, H.; Clausen, B. S. *Appl. Catal.* **1986**, *25*, 273−93.
(5) Farha, O. K.; Hupp, J. T. *Acc. Chem. Res.* **2010**, *43*, 1166−1175.
(6) Ferey, G. *Stud. Surf. Sci. Catal.* **2007**, *170A*, 66−86.
(7) Noro, S.-i.; Kitagawa, S. *Supramol. Chem. Org.-Inorg. Hybrid Mater.* **2010**, 235−269.
(8) Tranchemontagne, D. J.; Mendoza-Cortes, J. L.; O'Keeffe, M.; Yaghi, O. M. *Chem. Soc. Rev.* **2009**, *38*, 1257−1283.
(9) Farrusseng, D.; Aguado, S.; Pinel, C. *Angew. Chem., Int. Ed.* **2009**, *48*, 7502−7513.
(10) Ma, L.; Lin, W. *Top. Curr. Chem.* **2010**, *293*, 175−205.
(11) Corma, A.; Garcia, H.; Llabres i Xamena, F. X. *Chem. Rev.* **2010**, *110*, 4606−4655.
(12) Aguado, S.; Canivet, J.; Farrusseng, D. *J. Mater. Chem.* **2011**, *21*, 7582−7588.
(13) Lee, J. Y.; Farha, O. K.; Roberts, J.; Scheidt, K. A.; Nguyen, S. B. T.; Hupp, J. T. *Chem. Soc. Rev.* **2009**, *38*, 1450−1459.
(14) Phan, A.; Czaja, A. U.; Gandara, F.; Knobler, C. B.; Yaghi, O. M. *Inorg. Chem.* **2011**, *50*, 7388−7390.
(15) Jiang, H.-L.; Xu, Q. *Chem. Commun. (Cambridge, U. K.)* **2011**, *47*, 3351−3370.
(16) Jiang, H.-L.; Akita, T.; Ishida, T.; Haruta, M.; Xu, Q. *J. Am. Chem. Soc.* **2011**, *133*, 1304−1306.
(17) Gu, X.; Lu, Z.-H.; Jiang, H.-L.; Akita, T.; Xu, Q. *J. Am. Chem. Soc.* **2011**, *133*, 11822−11825.
(18) Dietzel, P. D. C.; Panella, B.; Hirscher, M.; Blom, R.; Fjellvag, H. *Chem. Commun.* **2006**, 959−961.
(19) Dietzel, P. D. C.; Johnsen, R. E.; Blom, R.; Fjellvag, H. *Chem.—Eur. J.* **2008**, *14*, 2389−2397.
(20) Millward, A. R.; Yaghi, O. M. *J. Am. Chem. Soc.* **2005**, *127*, 17998−17999.
(21) Wang, Z.; Cohen, S. M. *Chem. Soc. Rev.* **2009**, *38*, 1315−1329.
(22) Tanabe, K. K.; Cohen, S. M. *Chem. Soc. Rev.* **2011**, *40*, 498−519.
(23) Copéret, C.; Chabanas, M.; Saint-Arroman, R. P.; Basset, J.-M. *Angew. Chem., Int. Ed.* **2003**, *42*, 156−181.
(24) Liu, B.; Han, S.; Tanaka, K.; Shioyama, H.; Xu, Q. *Bull. Chem. Soc. Jpn.* **2009**, *82*, 1052−1054.
(25) Cychosz, K. A.; Wong-Foy, A. G.; Matzger, A. J. *J. Am. Chem. Soc.* **2009**, *131*, 14538−14543.
(26) Shi, F.; Hammoud, M.; Thompson, L. T. *Appl. Catal., B* **2011**, *103*, 261−265.
(27) Blanco-Brieva, G.; Campos-Martin, J. M.; Al-Zahrani, S. M.; Fierro, J. L. G. *Fuel* **2011**, *90*, 190−197.
(28) Britt, D.; Tranchemontagne, D.; Yaghi, O. M. *Proc. Natl. Acad. Sci. U. S. A.* **2008**, *105*, 11623−11627.
(29) Gandara, F.; Gutierrez Puebla, E.; Iglesias, M.; Proserpio, D. M.; Snejko, N.; Angeles Monge, M. *Chem. Mater.* **2009**, *21*, 655−661.
(30) Gandara, F.; Perles, J.; Snejko, N.; Iglesias, M.; Gomez-Lor, B.; Gutierrez-Puebla, E.; Monge, M. A. *Angew. Chem., Int. Ed.* **2006**, *45*, 7998−8001.
(31) Bonino, F.; Chavan, S.; Vitillo, J. G.; Groppo, E.; Agostini, G.; Lamberti, C.; Dietzel, P. D. C.; Prestipino, C.; Bordiga, S. *Chem. Mater.* **2008**, *20*, 4957−4968.
(32) Dietzel, P. D. C.; Besikiotis, V.; Blom, R. *J. Mater. Chem.* **2009**, *19*, 7362−7370.
(33) Dietzel, P. D. C.; Georgiev, P. A.; Eckert, J.; Blom, R.; Strassle, T.; Unruh, T. *Chem. Commun.* **2010**, *46*, 4962−4964.
(34) Vitillo, J. G.; Regli, L.; Chavan, S.; Ricchiardi, G.; Spoto, G.; Dietzel, P. D. C.; Bordiga, S.; Zecchina, A. *J. Am. Chem. Soc.* **2008**, *130*, 8386−8396.
(35) Chavan, S.; Vitillo, J. G.; Larabi, C.; Quadrelli, E. A.; Dietzel, P. D. C.; Bordiga, S. *Microp. Mesopor. Mater.* **2012**, in press, DOI:10.1016/j.micromeso.2011.07.025.
(36) Vitillo, J. G.; Groppo, E.; Bordiga, S.; Chavan, S.; Ricchiardi, G.; Zecchina, A. *Inorg. Chem.* **2009**, *48*, 5439−5448.
(37) Kaye, S. S.; Long, J. R. *J. Am. Chem. Soc.* **2008**, *130*, 806−807.
(38) Seisenbaeva, G. A.; Gohil, S.; Jansson, K.; Herbst, K.; Brorson, M.; Kessler, V. G. *New J. Chem.* **2003**, *27*, 1059−1064.
(39) Høj, M.; Linde, K.; Hansen, T. K.; Brorson, M.; Jensen, A. D.; Grunwaldt, J.-D. *Appl. Catal., A* **2011**, *397*, 201−208.
(40) Zhang, L.; Hu, Y. H. *J. Phys. Chem. C* **2010**, *114*, 2566−2572.